

**Thermal estimation of smartphone chipset:
mechanical distribution of chipset in
Multiphysics field**

Hanfeng Zhai

Department of Mechanics,
School of Mechanics and Engineering Science,
Shanghai University

March 8, 2020

Elastic Mechanics

Thermal estimation of smartphone chipset: mechanical distribution of chipset in Multiphysics field

Abstract

Chipset, a key essence that espouses the function of smartphone. The concentration of this study was to evaluate the thermal effect that was implemented to the chip.

Chipset was modeled as a thin plate and bonded by fixed support in the study. The governing equation was reasoned and demonstrated from the eigen-strain in Multiphysics field and constitutive equation. The boundary conditions of the chipset are given according to the physical circumstance in smartphones. Accordingly, coefficients and parameters was given by considering the real materials used in manufacturing. The stresses σ_{xx} and σ_{yy} , and displacements u_{xx} and u_{yy} distribution along the x and y axis is obtained and featured as graphs. The stresses are increasing successively along the x and y axis on chip. The displacements are increasing successively along the x and y axis. The deformed shape of chip under thermal effect is kindred to a trapezoid. A graphical distribution and numeral solution could be obtained by using finite element method. The stresses and displacements generally unevenly distributed in chip based on the simulation. Several possible optimization methods is discussed. These insights could provide guidelines for engineering and manufacturing of smartphone chip.

Keywords: smartphone chip; Multiphysics problem; finite element method; thermal analysis; stress field

Introduction

Smartphones are widely used and applied nowadays. With the growing trends of pursuing higher running speed with bigger storage, high functional and integrative chipset is required. However if the demand beyond the limitation of Strong heat flux and thermal displacement might seriously nullify the chip. Therefore, estimate the thermal effect that has implemented on chipset in smartphones' mechanical field is extremely important.

The thermal effect of chip has long been discussed and studied by scholars. Tang *et al.* [1] studied the thermal effect of chip's power enlarging functions observed through infrared rays. Liao *et al.* [2] concluded that Performance is affected by both temperature and supply voltage because of the temperature and voltage dependence of circuit delay through study the factors that may induce thermal runaway and leakage power and estimated the possible effects. Qian *et al.* [3] did an accurate and efficient thermal analysis for a VLSI chip is crucial, both for sign-off reliability verification and for design-time circuit optimization. Liang *et al.* [4] carried out a hybrid random walk method is proposed for the thermal analysis of integrated circuits.

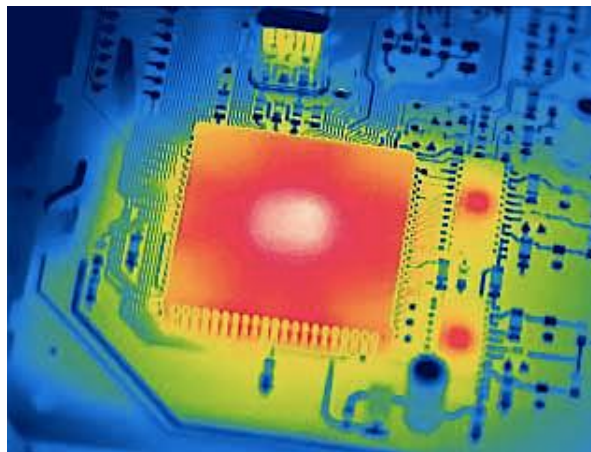


Fig. 1 Thermal image of chip under thermal field.

While when it comes to the mathematical estimation and simulation of the thermal loading on chip, Guo *et al.* [5] Aiming at the problem of local high-temperature thermal effects in large-scale IC chips, and developed a technique for thermal analysis of the chip using a random walk algorithm is proposed. Tang. *et al* [6] presented a present a hybrid algorithm to compute the convex hull of points in three or higher dimensional spaces through uses a GPU-based interior point filter to cull away many of the points that do not lie on the boundary. Plus, Ma *et al.* [7] also Aiming at the problem of local high-temperature thermal effects in large-scale IC chips, howbeit they proposed a grid-based random walk method to analyze the steady-state temperature distribution. Their algorithm only calculates the points near the heat source, thus the method greatly reduced the amount of calculation. Also, techniques based on the domain decomposition method (DDM) are presented for the 3-D thermal simulation of nonrectangular IC thermal model including heat sink and heat spreader by Yu *et al.* [8]. Zhan *et al.* [9] present three highly efficient thermal simulation algorithms for calculating the on-chip temperature distribution in a multilayered substrate structure.

Moreover, many scientists and scholars tried to experimentally analysis of the chip thermal process. Yu *et al.* [10] studied smartphone chipset's thermal performance not only by finite element simulation but also carried out experiments to reflect the thermal process of chip. Le *et al.* [11] describe the implementation of the IBM POWER6™ microprocessor, a two-way simultaneous multithreaded (SMT) dual-core chip whose key features include binary compatibility with IBM

POWER5™ microprocessor-based systems. They tested several properties of the chip and concluded that Key extensions to the coherence protocol enable POWER6 microprocessor-based systems to achieve better SMP scalability while enabling reductions in system packaging complexity and cost. In fine, the thermal effect of smartphone chip is at the central topic which attracted many scholars and studies.

Method

1. Mathematical Model

When loaded under Multiphysics field, the particle is undergoing both mechanical and non-mechanical effects. Therefore, estimating both these effects on materials requires both mechanics and physics field governing equations. In this problem, the chipset is modelled as a thin plate loaded under thermal field and bounded at the bottom side. The chipset model is simplified as below, where the heat is caused by battery.

Initially, converting the thermal effect into mechanical effect requires a mechanical tensor called the eigen-strain, which includes both the effects of volumetric and expansion strain due to physic field. Consequently, the thermal boundary conditions could be deduced and substitute it into the heat equation could reason the curvature of the plate. Subsequently, given the mechanical boundary conditions and substitute it into the Constitutive equation could reason the form of stress and displacement. By superpose the eigen-strain into the solution, the form of stresses and displacements are concluded.

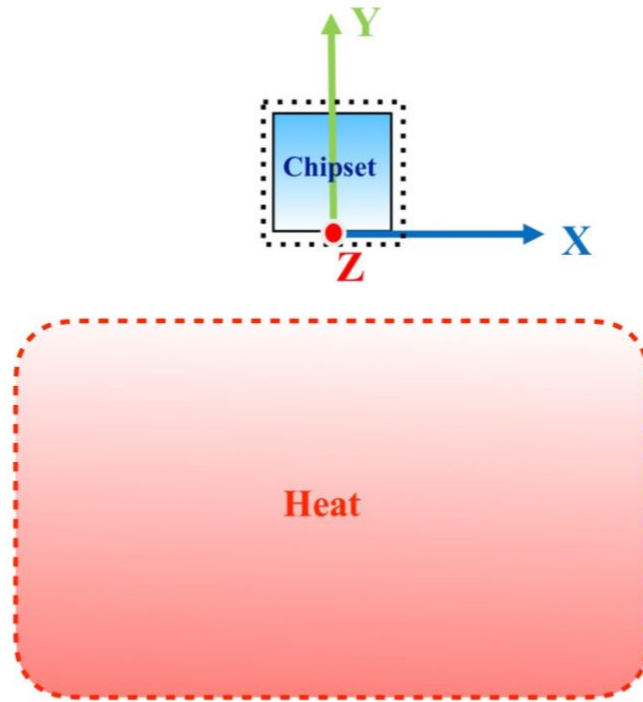


Fig. 2 The mechanical model of smartphone chipset physics, where the heat is created by the exothermic process of battery. In the mechanical model, the battery thermal field is considered as a semi-infinite heating source.

1) Eigen-strain:

Eigen-strain consists of two parts: volumetric strain and expansion strain.

Volumetric strain: the materials' volume change under free-standing condition

$$\varepsilon_V = \frac{\Delta V}{V_0} = \alpha(T - T_0)$$

Where α is called the volumetric thermal expansion coefficient. T_0 is the initial temperature.

Expansion strain: the materials' expansion or shrink caused by change of temperature.

$$\varepsilon_{11} = \alpha_{11}(T - T_0), \quad \varepsilon_{ij} = \alpha_{ij}(T - T_0).$$

for isotropic material: $\alpha_{11}=\alpha_{22}=\alpha_{33}=\frac{1}{3}\alpha$. We may name these strains induced by physical variables other than the stress the eigen-strain, denoted by ε^* , ε_{ij}^* . It is the strain caused by physical changes under stress-free condition.

2) Heat equation:

For thermal field, the relationship between temperature and time is

$$\frac{\partial T}{\partial t} - \frac{k}{\rho c_p} \nabla^2 T = 0$$

where c_p is the specific heat capacity, ρ is the mass density of the material and k is the thermal conductivity.

In this case, the temperature boundary condition of chipset could be given

i) Temperature on boundary: $T = -5000 \cdot y + 345.15[\text{K}]$ on S

ii) Heat flux boundary condition: $\frac{\partial T}{\partial n} = 0$, on S

iii) Convection boundary condition (Newton boundary condition):

$$\frac{\partial T}{\partial n} = h(T - T_0) \text{ on } S, \text{ where } h \text{ is film coefficient, } T_0 = 295.15\text{K.}$$

3) Constitutive equations

Considering the Multiphysics field, Hooke's law for elastic mechanical displacements needs to be generalized to take into account eigen-strain which is caused by other physical variables.

For smartphones' chipset, a thin plate is loaded in multiaxial state, where

$$\sigma_{ij} \neq 0 \ (i,j=1,2,3)$$

$$\left\{ \begin{array}{l} \varepsilon_{11} = \frac{1}{E} \sigma_{11} - \frac{1}{E} \sigma_{22} - \frac{1}{E} \sigma_{33} + \frac{1}{3} \alpha(T - T_0) \\ \varepsilon_{22} = \frac{1}{E} \sigma_{22} - \frac{1}{E} \sigma_{11} - \frac{1}{E} \sigma_{33} + \frac{1}{3} \alpha(T - T_0) \\ \varepsilon_{33} = \frac{1}{E} \sigma_{33} - \frac{1}{E} \sigma_{22} - \frac{1}{E} \sigma_{11} + \frac{1}{3} \alpha(T - T_0) \\ \varepsilon_{12} = \frac{1}{2G} \sigma_{12} \\ \varepsilon_{13} = \frac{1}{2G} \sigma_{13} \\ \varepsilon_{23} = \frac{1}{2G} \sigma_{23} \end{array} \right.$$

which could be simplified as

$$\varepsilon_{ij} = \frac{1 + \nu}{E} \sigma_{ij} + \frac{\nu}{E} \sigma_{kk} \delta_{ij} + \varepsilon_{ij}^*$$

where $\varepsilon_{ij}^* = \frac{1}{3} \alpha(T - T_0) \delta_{ij}$.

Thence, substitute strain and eigen-strain into Hooke's law, one could obtain the stress components in terms of strain components:

$$\sigma_{ij} = 2G(\varepsilon_{ij} - \varepsilon_{ij}^*) + \frac{E\nu}{(1 + \nu)(1 - 2\nu)} (\varepsilon_{kk} - \varepsilon_{kk}^*)$$

Boundary Condition:

Mechanical condition:

- i) Displacement boundary condition: $u_i = 0$ on S_n
- ii) Traction boundary condition: $\sigma_{jinj} = 0$ on S_n

The simplified model of the chipset is shown as below in Figure 3.

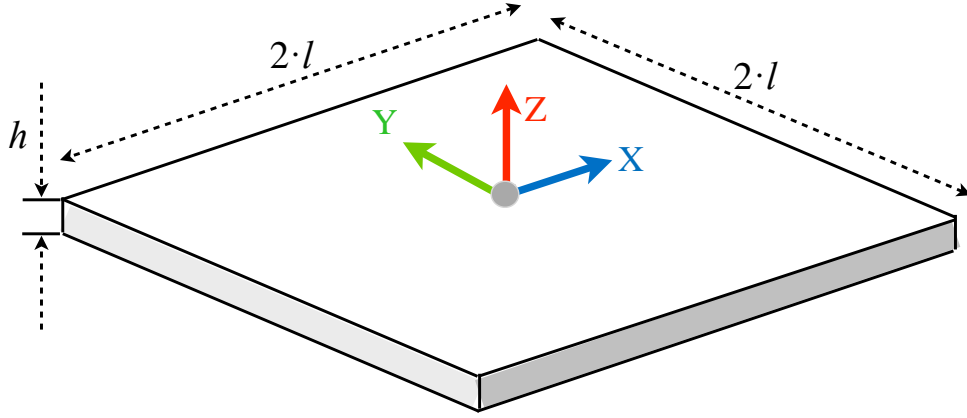


Fig. 3 The size parameters and three-dimensional simplified model of the chipset, where $l=0.005\text{m}$, $h=0.001\text{m}$.

Based on the given boundary conditions, it could be induced that in thermal field:

$$\sigma_{yy} \neq \sigma_{xx} \neq 0;$$

$$\sigma_{zz} = \sigma_{xy} = \sigma_{yz} = \sigma_{xz} = 0;$$

Therefore, the eigenstrain could be deduced:

$$\varepsilon_{zz} = -\frac{\nu}{E}\sigma_{xx} - \frac{\nu}{E}\sigma_{yy} + \varepsilon_{zz}^*$$

$$\varepsilon_{xx} = \varepsilon_{x0} + \kappa y$$

$$\varepsilon_{yy} = \varepsilon_{y0} + \kappa y$$

Thence, we could give the form of σ_{xx} and σ_{yy} :

$$\begin{aligned}\sigma_{xx} &= \frac{E}{1+\nu}(\varepsilon_{xx} - \varepsilon_{xx}^*) + \frac{E\nu}{(1+\nu)(1-2\nu)}(2\varepsilon_{xx} - \frac{\nu}{E}\sigma_{xx} - \frac{\nu}{E}\sigma_{yy} - 2\varepsilon_{xx}^*) \\ \sigma_{yy} &= \frac{E}{1+\nu}(\varepsilon_{yy} - \varepsilon_{yy}^*) + \frac{E\nu}{(1+\nu)(1-2\nu)}(2\varepsilon_{yy} - \frac{\nu}{E}\sigma_{xx} - \frac{\nu}{E}\sigma_{yy} - 2\varepsilon_{yy}^*)\end{aligned}$$

Consequently, we substitute the above simultaneous equations:

$$\begin{aligned}\sigma_{xx} &= \frac{E - E\nu - E\nu^2}{(1-\nu^2)(1-2\nu)}(\varepsilon_{xx} - \varepsilon_{xx}^*) - \frac{E\nu^2}{(1-\nu^2)(1-2\nu)}(\varepsilon_{yy} - \varepsilon_{yy}^*) \\ \sigma_{yy} &= \frac{E - E\nu - E\nu^2}{(1-\nu^2)(1-2\nu)}(\varepsilon_{yy} - \varepsilon_{yy}^*) - \frac{E\nu^2}{(1-\nu^2)(1-2\nu)}(\varepsilon_{xx} - \varepsilon_{xx}^*)\end{aligned}$$

Based on the strains, one could also obtain the displacement:

$$u_{ij} = \int \varepsilon_{ij} dx_i$$

Subsequently, in order to simplified the calculation process, we name $\frac{E-E\nu-E\nu^2}{(1-\nu^2)(1-2\nu)}$ as A , $\frac{E\nu^2}{(1-\nu^2)(1-2\nu)}$ as B .

The traction-free boundary conditions on two side faces have been satisfied automatically. Since we focus on the eigen-strain induced stress which does not include the effect of external mechanical loading the end of plate is mechanically free and the mechanical boundary conditions could be specified as

$$\int_{-l}^l \sigma_{xx} dy = 0, \quad \int_{-l}^l \sigma_{yy} dy = 0$$

$$\int_{-l}^l \sigma_{yy} y dy = 0$$

Substitute the above form of σ_{xx} and σ_{yy} into the boundary conditions:

$$A \cdot 2l \cdot \varepsilon_{y0} - A \cdot \int_{-l}^l \varepsilon_{yy}^* dz - B \cdot 2l \cdot \varepsilon_{x0} + B \cdot \int_{-l}^l \varepsilon_{xx}^* dz = 0$$

$$A \cdot 2l \cdot \varepsilon_{x0} - A \cdot \int_{-l}^l \varepsilon_{yy}^* dz - B \cdot 2l \cdot \varepsilon_{y0} + B \cdot \int_{-l}^l \varepsilon_{xx}^* dz = 0$$

$$A \cdot \int_{-l}^l (\varepsilon_{y0} + \kappa y) y dy - A \cdot \int_{-l}^l \varepsilon_{yy}^* y dy - B \cdot \int_{-l}^l (\varepsilon_{x0} + \kappa y) y dy + B \cdot \int_{-l}^l \varepsilon_{xx}^* y dy = 0$$

In order to simplify the calculation process, we elicit the given forms:

$$A \cdot 2h = m, B \cdot 2h = n$$

By solving the above equations, we could obtain the parameters in the equations:

$$\varepsilon_{x0} = \frac{A-B}{m-n} \left(\int_{-l}^l \varepsilon_{xx}^* dy + \int_{-l}^l \varepsilon_{yy}^* dy \right) - \varepsilon_{y0}$$

$$\begin{aligned}
 \varepsilon_{x0} &= \frac{A-B}{m-n} \left(\int_{-l}^l \varepsilon_{xx}^* dy + \int_{-l}^l \varepsilon_{yy}^* dy \right) - \frac{A}{m+n} \int_{-l}^l \varepsilon_{yy}^* dy \\
 &\quad + \frac{B}{m+n} \int_{-l}^l \varepsilon_{xx}^* dy - \frac{(A-B)n}{m^2-n^2} \left(\int_{-l}^l \varepsilon_{xx}^* dy + \int_{-l}^l \varepsilon_{yy}^* dy \right) \\
 \varepsilon_{y0} &= \frac{A}{m+n} \cdot \int_{-l}^l \varepsilon_{yy}^* dy - \frac{B}{m+n} \int_{-l}^l \varepsilon_{xx}^* dy + \frac{(A-B)n}{m^2-n^2} \left(\int_{-l}^l \varepsilon_{xx}^* dy + \int_{-l}^l \varepsilon_{yy}^* dy \right) \\
 \kappa &= \frac{3(A \cdot \int_{-l}^l \varepsilon_{yy}^* y dy - B \cdot \int_{-l}^l \varepsilon_{xx}^* y dy)}{(A-B) \cdot 2h^3}
 \end{aligned}$$

Hence, the stress σ_{xx} and σ_{yy} is obtained.

Now we substitute the eigen-strain $\varepsilon_{xx}^*(z) = \frac{1}{3}\alpha T(z)$, $\varepsilon_{yy}^*(z) = \frac{1}{3}\alpha T(z)$, we have

$$\begin{aligned}
 \varepsilon_{x0} &= \frac{\alpha}{3h} \int_{-l}^l T(y) dy + \frac{\alpha(B-A)}{6h(A+B)} \int_{-l}^l T(y) dy - \frac{\alpha B}{3h(A+B)} \int_{-l}^l T(y) dy \\
 \varepsilon_{y0} &= \frac{\alpha(A-B)}{6h(A+B)} \cdot \int_{-l}^l T(y) dy + \frac{\alpha B}{3h(A+B)} \int_{-l}^l T(y) dy \\
 \kappa &= \frac{\alpha \cdot \int_{-l}^l T(y) y dy}{2h^3}
 \end{aligned}$$

Therefore, the final form of the stress is reasoned by substitute ε_{x0} , ε_{y0} , κ into the equation of stress and displacement.

Subsequently, substitute the given temperature and coefficients into the stress and displacement.

Temperature: $T(y) = -5000y + 345.15$ [K]

Volumetric thermal expansion coefficient: $\alpha(\text{Si}) = 5.8 \times 10^{-7}$ [1/K]

For silicon (100) and (110), Young's modulus varies from 130.2 GPa to 187.5 GPa, Poisson's ratio varies from 0.064 to 0.361. Therefore, we let $E(\text{Si}) = 150$ [GPa] and $\nu(\text{Si}) = 0.1$.

The results is obtained by substituting these coefficients.

2. Finite Element Simulation

To analyzing this problem more comprehensively and better observing the mechanical change of the chipset, operating a numerical simulation based on ANSYS could offer a reference on the given calculation. To estimate the details more accurately, I model the major structures of battery, screen, and circuit board to bond with the chipset. In the modelling, the material for battery is Copper; the material for circuit board is High Polymer (a kind of plastic); the material for screen is glass; the material for chipset is Silicon. The model is shown in Figure 4.

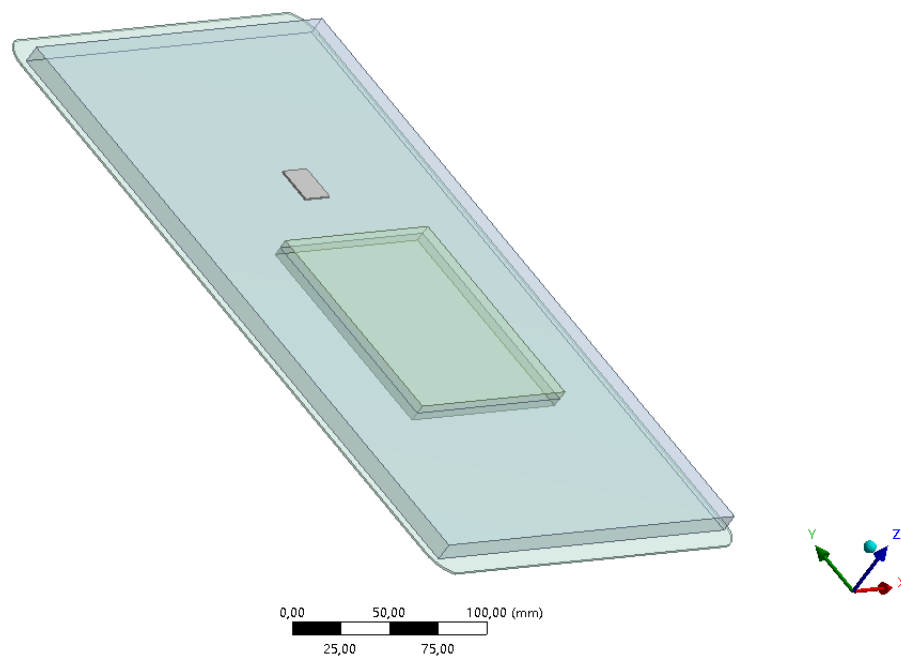


Fig. 4 The modelling of the chipset and its corresponding parts in smartphone. The bottom part is smartphone's screen. The large cuboid is the circuit board. The small cuboid is the battery. The small slice is the chipset.

Results

1. Mechanical Variables

As it is shown in the former chapter, after substituting the results of strain, eigen-strain and curvature into the form of the stress and displacement, the final results of

these mechanical variables is deduced. However due to the form of the results is complex and cannot be written as algorithm forms, featuring these variables as graphs is more intuitive and clearheaded.

Initially, the high temperature of the battery in the smartphone is considered as a semi-infinite thermal field. For areas surround the chipset, the thermal field is considered as a successively decreasing temperature, where the schematic diagram is shown in Figure 5, the graph is shown in Figure 6.

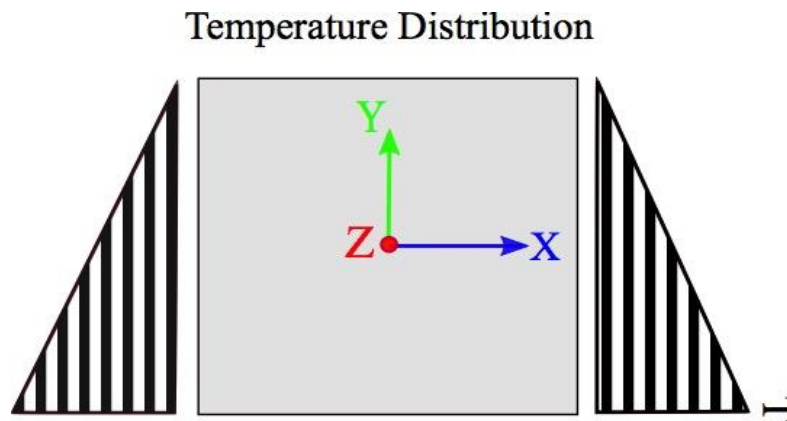


Fig. 5 The temperature distribution along the chipset when loaded under the thermal effect of smartphone battery. In this problem, the temperature function is considered as a linear equation ($T(y) = -5000 \cdot y + 345.15$ [K]) of y axis to temperature.

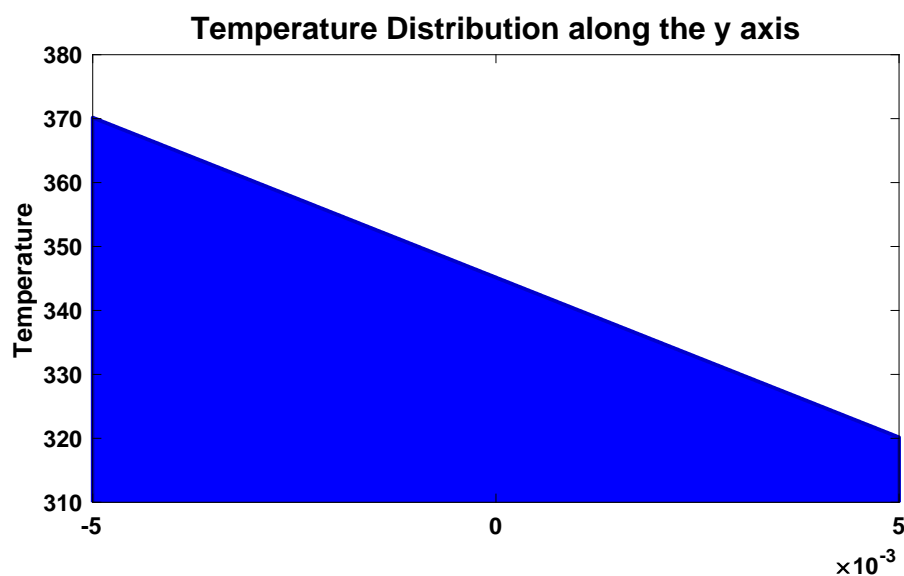


Fig. 6 The plotted graph of y axis to temperature.

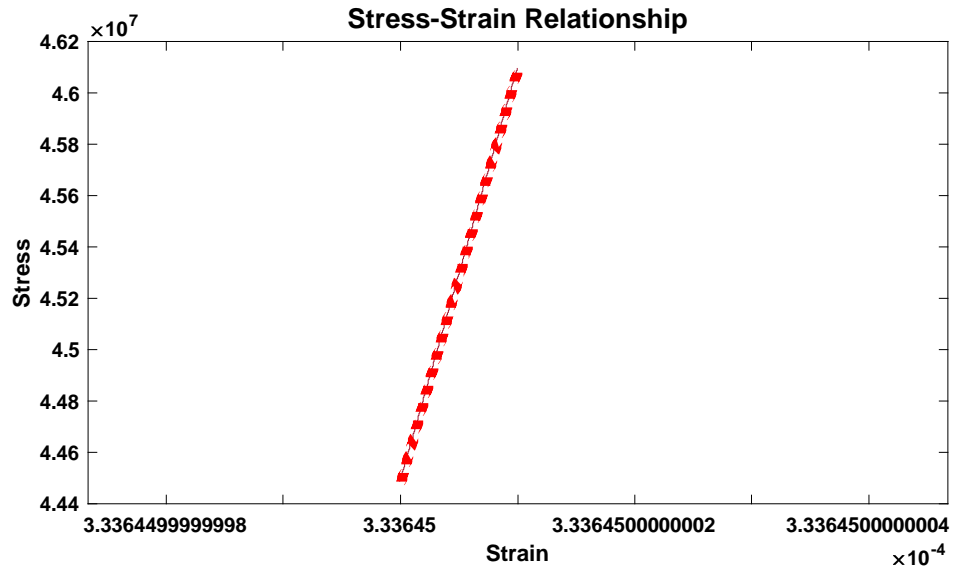


Fig. 7 The stress-strain diagram representing the constitutive equation.

After substitute the temperature equations into the stress and displacement equations, graphical features and the two stresses σ_{xx} and σ_{yy} along the y axis is shown in Figure 8(a), and the separate graphs of each stresses is shown in Figure 8(b).

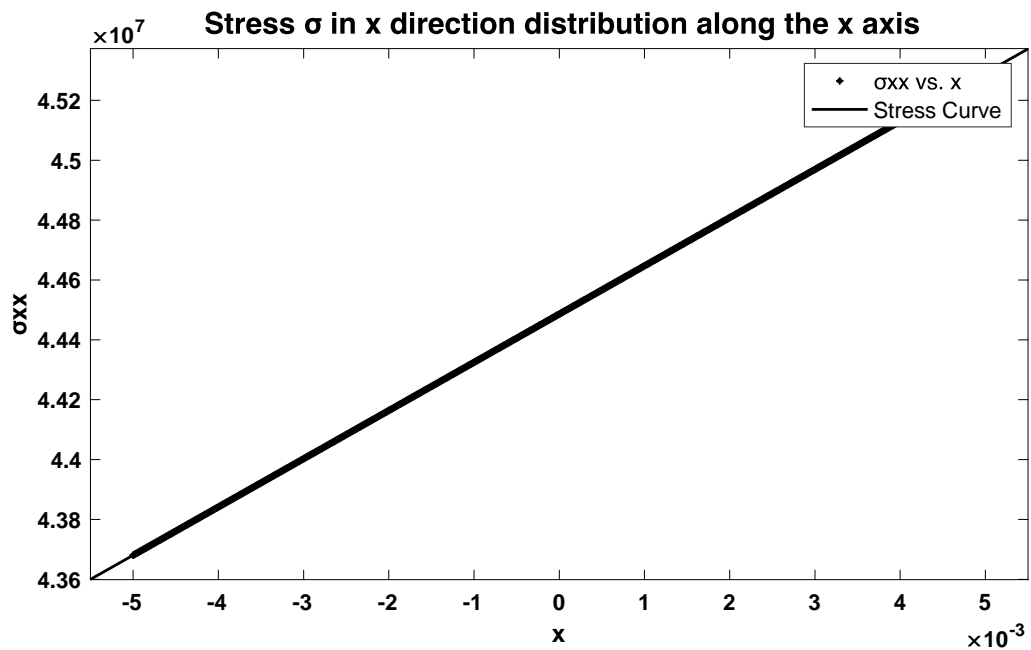


Fig. 8 (a) Relationship of stress σ_{xx} to x axis.

As it is shown in Figure 8(a) and (b), the stress shows a linear relation with the distribution axis, which shows that stress is growing along the chip.

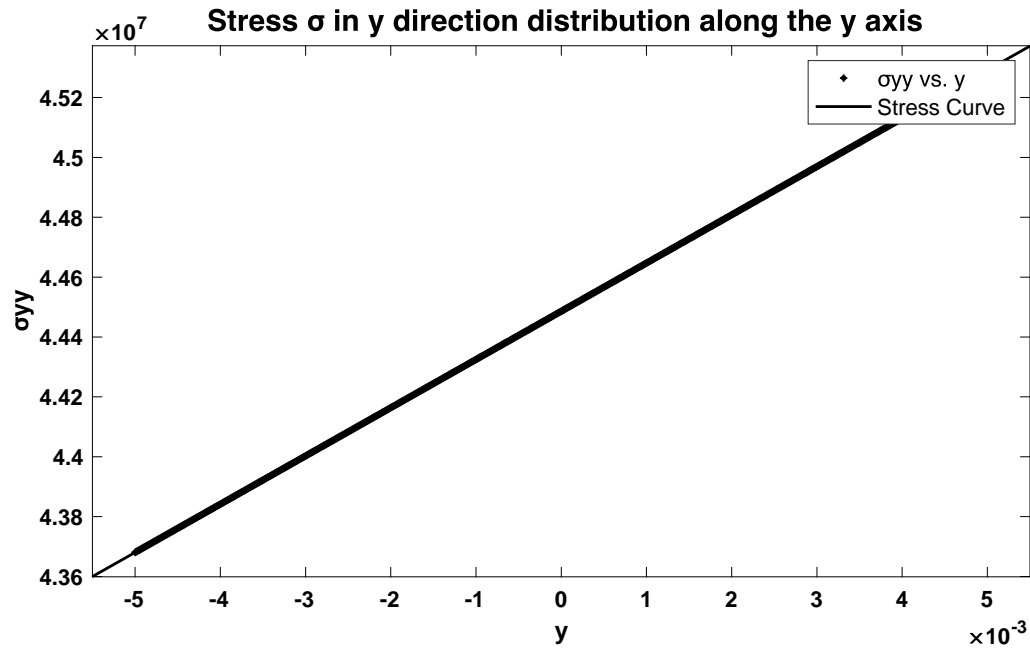


Fig. 8 (b) Relationship of stress σ_{yy} to y axis.

Stress σ_{xx} distribution along the chip

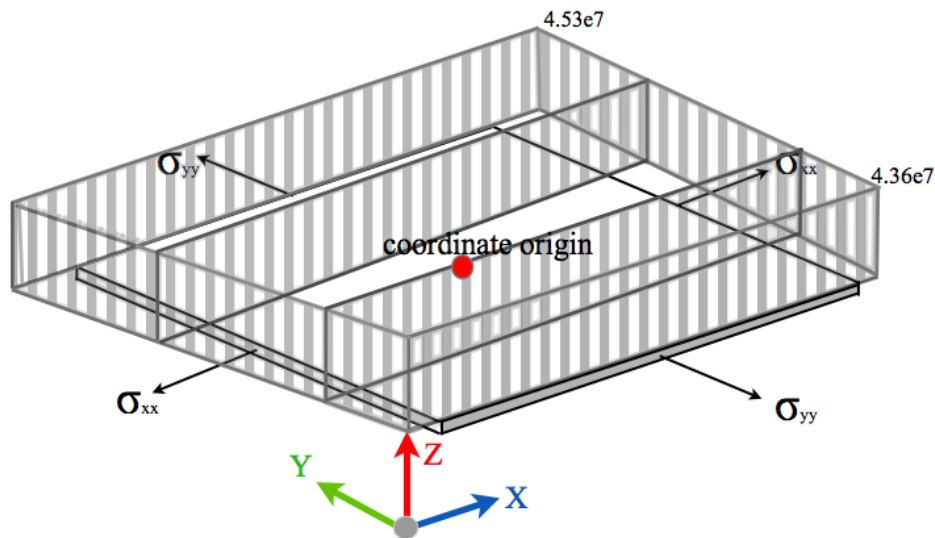


Fig. 8 (c) The distribution of stress σ_{xx} on smartphone chip.

Stress σ_{yy} distribution along the chip

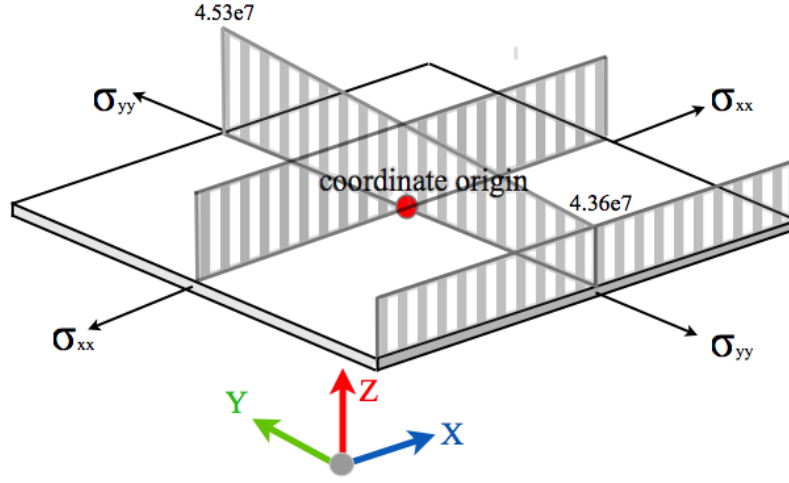


Fig. 8 (d) The distribution of stress σ_{yy} on smartphone chip.

From the figures obtained one can deduce that the stresses σ_{xx} and σ_{yy} along the y axis are both increasing successively. In the shown graphs and calculated equations, one knows that stress σ_{xx} and σ_{yy} remains a constant on x axis and satisfy a linear relation with the y axis. From the obtained diagram one could plot the stress σ_{xx} and σ_{yy} distribution on the smartphone chip, respectively [Figure 8(c) and Figure 8(d)].

Similar to the stresses, the displacement could also be calculated through substituting the strain into strain-displacement relation $u_{ij} = \int \varepsilon_{ij} dx_i$. The graphical feature of the two displacements are shown as below. Based on equation given above: $\varepsilon_{xx} = \varepsilon_{x0} + \kappa y$, $\varepsilon_{yy} = \varepsilon_{y0} + \kappa y$. We obtain that the both the strain in x direction and y direction satisfies a linear relation with variable y. Thence through integration we deduce that the displacement in x direction is a function consists of both variables x and y. Simultaneously, the displacement in y direction obeys a quadratic relation.

By featuring the two displacements u_{xx} and u_{yy} one could deduce that the two displacements are following the same trend. They both initiated with the negative values and values zero at the central point and increasing successively.

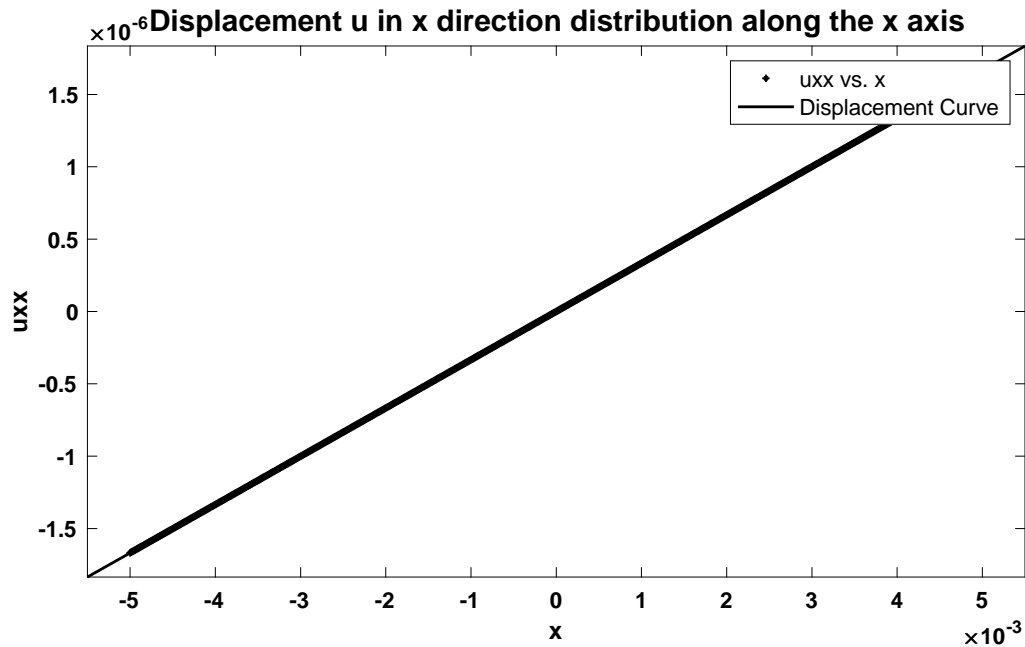


Fig. 9 (a) Relationship of stress u_{xx} to x axis.

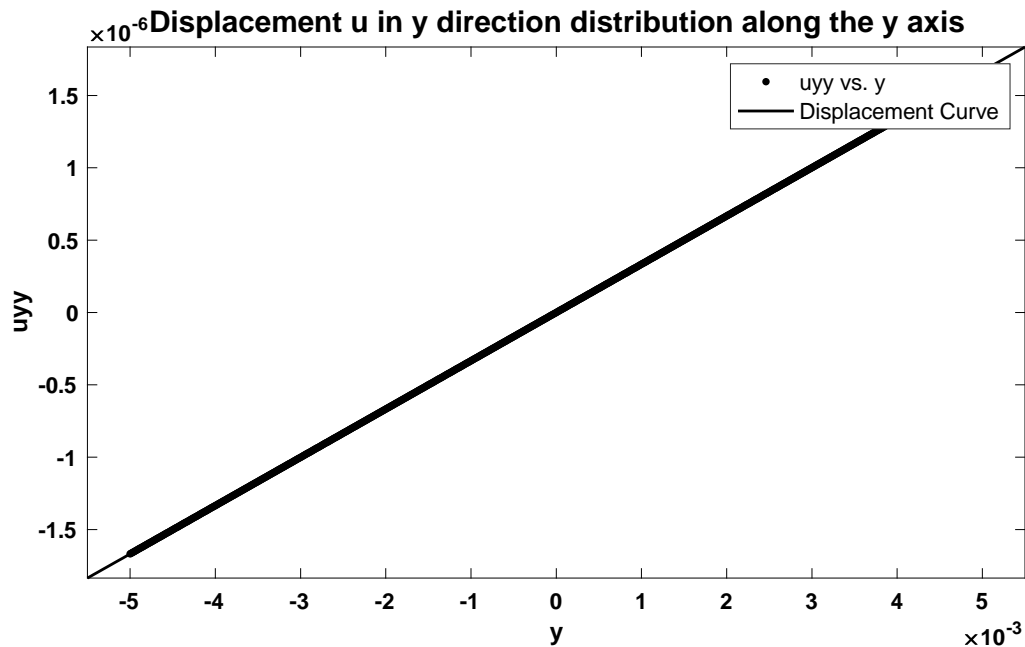


Fig. 9 (b) Relationship of stress u_{yy} to y axis.

Based on the equation calculated from the integration and deducing mentioned before one could plot the displacement diagrams as shown in Figure 9(a) and (b). Plus, a three-dimensional relation of the displacements to the axis and temperature [Figure 9(c)] and displacements to the two axes [Figure 9(d)].

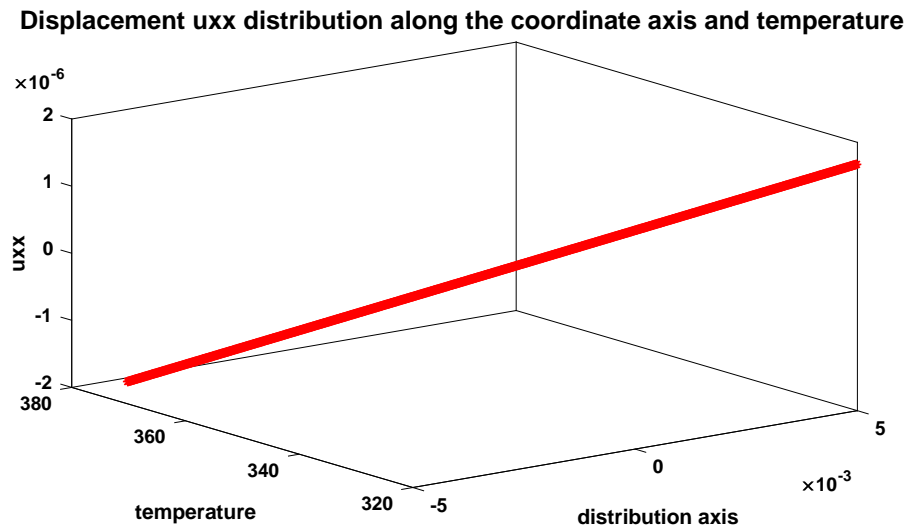


Fig. 9 (c) Relationships between displacement to the distribution axis (x or y) and temperature.

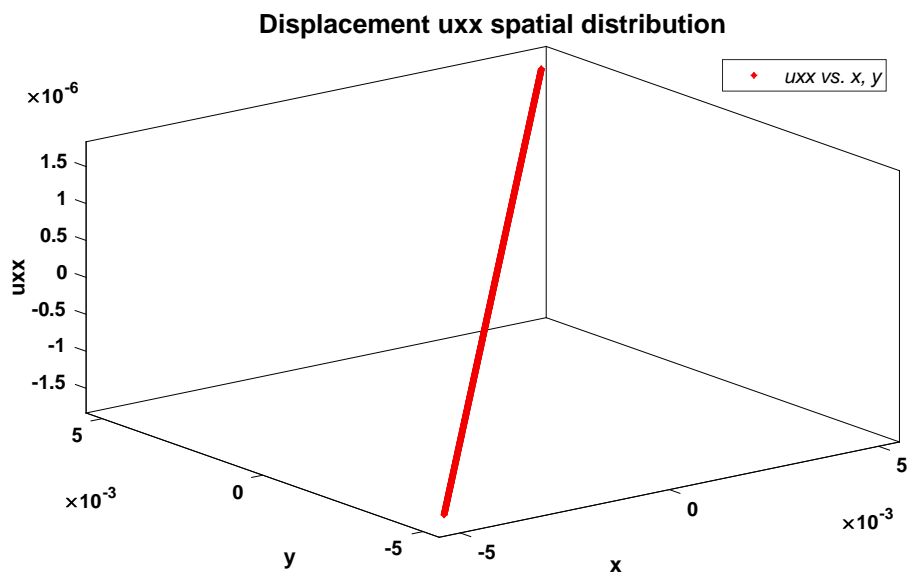


Fig. 9 (d) The spatial distribution of the displacement u_{xx} .

Based on the plot diagrams containing relations between displacement u_{xx} and u_{yy} to the two axes we could build schematic view of displacement distribution on the smartphone chip as shown in Figure 9(e) and Figure 9(f).

Displacement u_{xx} distribution along the chip

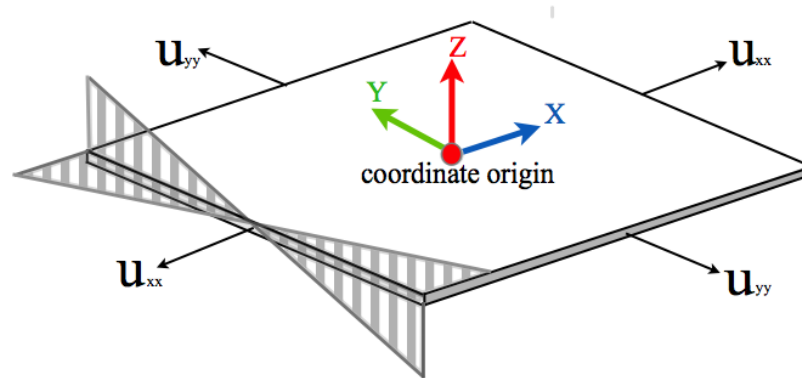


Fig. 9 (e) The distribution of displacement u_{xx} on smartphone chip.

Displacement u_{yy} distribution along the chip

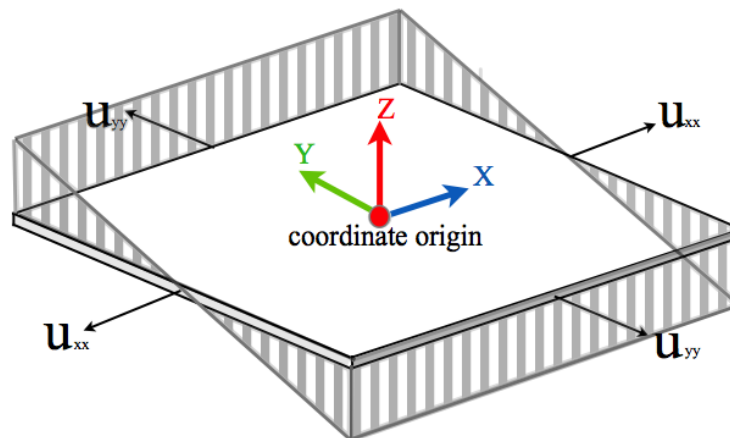


Fig. 9 (f) The distribution of displacement u_{yy} on smartphone chip.

2. Finite Element Estimation

As it is modelled in Figure 4, we set the temperature of the battery is 70°C (345.15K) and simulate both the temperature field, stress and displacement field. The results is shown is Figure 10(a), Figure 10(b), Figure 10(c).

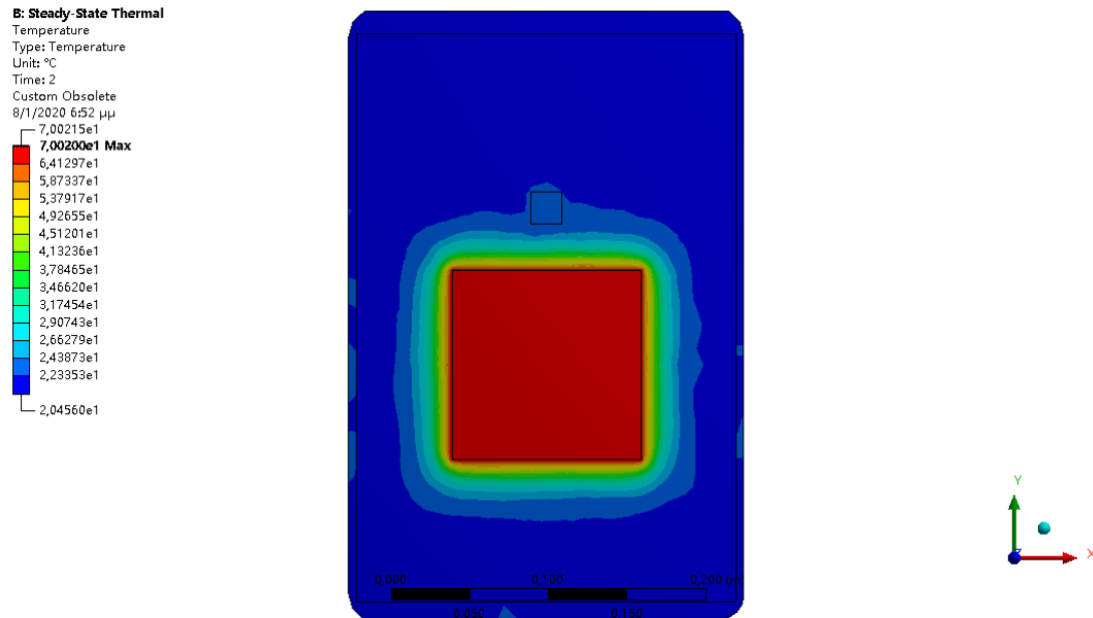


Fig. 10 (a) The temperature distribution of simulation in smartphones when battery is set to be at 345.15K .

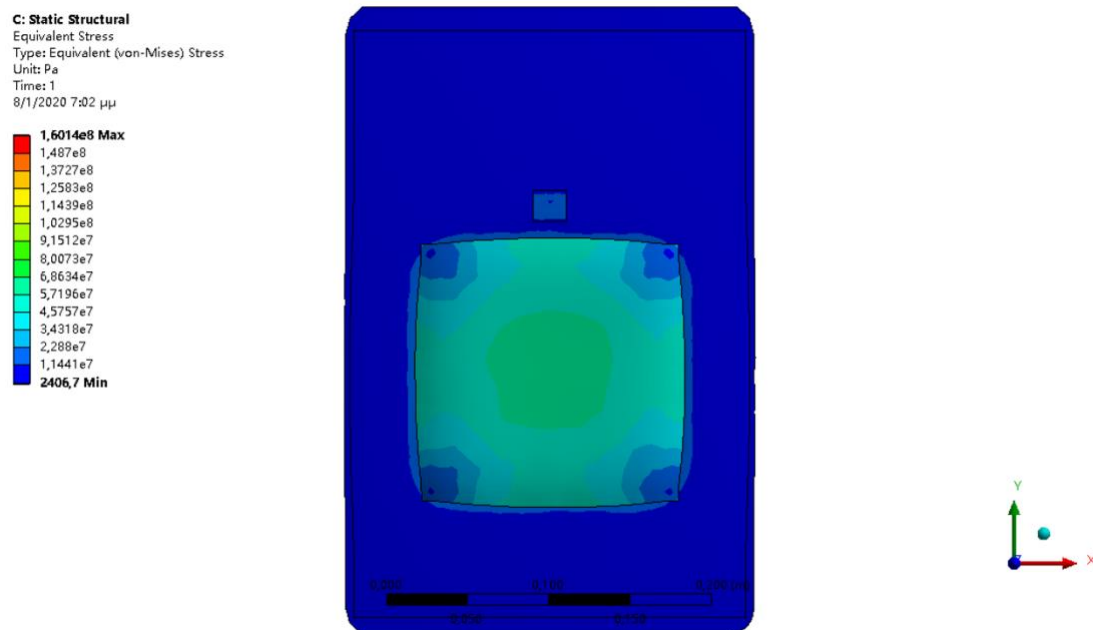


Fig. 10 (b) The stress distribution of simulation in smartphones when battery is set to be at 345.15K .

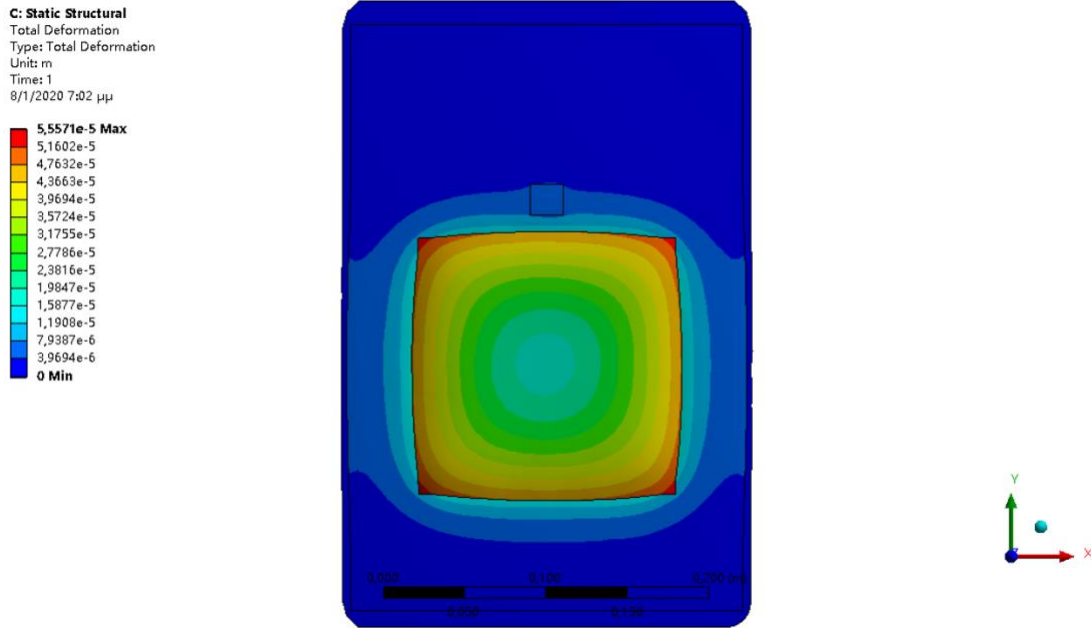


Fig. 10 (c) The displacement distribution of simulation in smartphones when battery is set to be at 345.15K.

According to the simulation results shown above, one could obtain that from the interaction of the temperature, the chip temperature is generally higher than its surrounding circuit board. The temperature of the chip is around 25°C to 30°C, which is not a high considering the heat of the battery.

From the result of stress, one could observe that the stress is not evenly distributed along the chip, where the central part has generally higher stress value than the chip's edge. Along the y axis, the stress on lower part is trivially higher than the stress on higher part, which correspond perfectly to the calculation results. The stress value is around $2.3 \times 10^7 \text{Pa}$.

From the displacement results, one can obtain that the displacement is not uniformly distributed along the y axis, where the value is around $3.96 \times 10^{-6} \text{m}$. The deformed shape looks like a trapezoid, which shows that the chip tend to extend its volume when encounters higher temperature.

Conclusion

In determining the stress and displacement of smartphone chipset, I assume the temperature distribution is a linear equation along the y axis, where the equation is $T = -5000 \cdot y + 345.15[\text{K}]$. The mathematical solution of the stresses and displacement is obtained through substitute the strain and eigen-strain into the heat equation and constitutive equation. By implementing the thermal load into the stress and displacement results calculated, one could plot the stress-x, stress-y and displacement-x, displacement-y diagrams [Figure 8(a), (b). Figure9(a), (b)]. Furthermore, schematic view of stresses distribution on smartphone chip is given based on graphs [Figure 8(c), (d)]. A spatial distribution of displacement u_{xx} to temperature and axis [Figure 9(c)] and the spatial distribution of u_{xx} [Figure 9(d)] can be plotted. Similarly, schematic views showing the displacements distribution on smartphone chip is given based on the calculated results [Figure 9(e) and Figure 9(f)].

From the simulation, one could model the chip bonded with circuit board and battery, screen. The simulation results shows that chip temperature is approximately 25-30°C when battery is 70°C.

Based on the simulation results, the stress is not uniformly distributed along the y axis on chip, which corresponds to the mathematical result. the stress value on chip is approximately $2.3 \times 10^7 \text{Pa}$ [Figure 10(b)]. The displacement is also not uniformly distributed along the y axis, where the displacement value is approximately $3.96 \times 10^{-6} \text{m}$ [Figure 10(c)]. Through enlarging the schematic view of the chip, one could observe that the deformed shape of the chip is kindred to a trapezoid.

Discussion

In real situation, there are a significant amount of nanoscale or microscale circuits, including memory cells and sensing circuitry that carved on the chip. These connections proffer the hardware to support the smartphone functions. What's more, these circuits are extremely sensitive for changes of its physical circumstances.

Based on stress results, one could observe that stresses increase successively along the x and y axis following a linear relation. To prevent disfunction caused by the relatively high temperature, several optimizations could be carried out for chip such as adding a thermal segregation layer in chip, using materials that resist suppression on x axis howbeit resist extension on y axis, etc.

Based on displacement results, one could observe that displacements also increase successively along the x and y axis, in which the displacement in x direction satisfy a linear relation and displacement in y direction satisfy a quadratic relation. Similar to stress estimation, one could also carry out several actions to optimize the chip such as make small changes on the original shape of chip to prevent possible displacement caused by temperature change, using anisotropic materials as mentioned in the last paragraph, etc.

Eventually, specific optimization method should be advised from people who expert in electronic engineering based on these results. From the mechanic's perspective, I could only offer reasonable conjecture based on the results. These results could provide reference in smartphones' chips design and manufacturing.

References

- [1] Tang Sha, Wang Zhizhe, Chen Yongfan. Discussion on infrared thermal analysis of power amplifier chip. *Reliability and Environmental Tests of Electronic Products*, 2019, 37(05):63-67.
- [2] Weiping Liao, Lei He, K.M. Lepak Temperature and supply Voltage aware performance and power modeling at microarchitecture level. *IEEE Transactions on Computer-Aided Design of Integrated Circuits and Systems*, 2005, Vol.24 (7), pp.1042-1053
- [3] Haifeng Qian, Sachin S. Sapatnekar, Eren Kursun. Fast poisson solvers for thermal analysis. *ACM Transactions on Design Automation of Electronic Systems (TODAES)*. 2012(3)
- [4] Liang Yuan, Yu Wenjian, Qian Haifeng. A hybrid random walk algorithm for 3D thermal analysis of integrated circuits. *Proc of Asia and South Pacific Design Automation Conference*. 2014
- [5] Guo Jun, Dong Sheqin. Application of Random Walk Algorithm in Thermal Analysis of IC Chip[J]. *Journal of Computer-Aided Design and Computer Graphics*, 2010, 22(04):689-694.
- [6] Min Tang, Jie-yi Zhao, Ruo-feng Tong, Dinesh Manocha. GPU accelerated convex hull computation[J]. *Computers & Graphics*, 2012, 36(5).
- [7] Ma.J, Xu.N. Research on GPU Thermal Analysis Method Based on GPU[J]. *Application Research of Computers*, 2018, 35(03):773-776.
- [8] Yu Wenjian, Zhang Tao, Yuan Xiaolong, et al. Fast 3D thermal simulation for integrated circuits with domain decomposition method. *IEEE Transactions on Computer Aided Design of Integrated Circuits and Systems*. 2013
- [9] Zhan, Yong, Sapatnekar, Sachin S. High-efficiency green function-based thermal simulation algorithms. *IEEE Transactions on Computer Aided Design of Integrated Circuits and Systems*. 2007
- [10] Youmin Yu, Nader Nikfar, Todd Sutton, Impact of Chipset Configuration on Thermal Performance of Smartphones, 2018 17th IEEE Intersociety Conference on Thermal and Thermomechanical Phenomena in Electronic Systems (ITherm)
- [11] Le, Hung Q, Starke, William J., Fields, J. Stephen, O'Connell, Francis P., Nguyen, Dung Q., Ronchetti, Bruce J., Sauer, Wolfram M., Schwarz, Eric M., Vaden, Michael T. IBM POWER6 microarchitecture. *IBM Journal of Research and Development* . 2007